IL NUOVO CIMENTO VOL. 20 C, N. 5 Settembre-Ottobre 1997

Cosmological evolution of extragalactic sources in the infrared and contributions to the background radiation(*)

G. DE ZOTTI(1), A. FRANCESCHINI(2), P. MAZZEI(1)
G. L. GRANATO(1) and L. DANESE(3)

(1) *Osservatorio Astronomico - Vicolo dell'Osservatorio 5, I-35122 Padova, Italy*
(2) *Dipartimento di Astronomia, Università di Padova*
Vicolo dell'Osservatorio 5, I-35122 Padova, Italy
(3) *SISSA - International School for Advanced Studies*
Strada Costiera 11, I-34014 Trieste, Italy

(ricevuto il 5 Dicembre 1996; approvato il 27 Febbraio 1997)

Summary. — Infrared surveys provide essential insights on galaxy evolution. If near-IR studies suggest a mild evolution of stellar populations with cosmic time, indications of a substantial evolution have been seen in the far IR, although the available information is largely insufficient to delineate precise evolutionary properties. A consistent picture encompassing all the currently available data may be obtained assuming that dust extinction hides the early evolutionary phases of spheroidal galaxies in the optical band, while the corresponding dust re-radiation in the far IR may have been, during the early evolutionary phases, orders of magnitude larger than today. Hyperluminous IRAS galaxies might be extreme examples of this situation. Additional indications that at least some spheroidal galaxies may have been very dusty during their early evolution are provided by recent data on high redshift radio galaxies and quasars. Galaxies are the likely dominant contributors to the IR background. However, in the framework of unified models for Active Galactic Nuclei, a large number of nuclei hidden by a dusty torus may be expected. Implications for the IR background are discussed.

PACS 96.40 – Cosmic rays.
PACS 98.52 – Normal galaxies; extragalactic objects and systems (by type).
PACS 01.30.Cc – Conference proceedings.

1. – Galaxy evolution in the optical-IR. General observational trends

Optical surveys have constituted for many years the primary tool to investigate the photometric evolution of galaxies, reflecting the evolution of stellar populations. CCD detectors have allowed to reach extremely faint magnitudes, down to $B \simeq 27$–28, *i.e.* to

(*) Paper presented at the VII Cosmic Physics National Conference, Rimini, October 26-28, 1994.

surface densities as high as $\simeq 3 \times 10^5$ galaxies degrees^{-2}. A remarkable excess over a smooth extrapolation from brighter magnitudes was observed in the B-band counts, beginning at $B \simeq 20$ and continuing to the faintest levels.

Counts and colors indicated a substantial increase with look-back time of the surface density of blue galaxies, consistent with evolutionary stellar population synthesis models provided that the universe has a low density ($q_0 \simeq 0.05$) and galaxies form at high redshifts ($z_{\rm for} \simeq 30$).

The observed redshift distributions of galaxies down to $B \simeq 22$–24, however, cannot be accounted for by pure luminosity evolution models, at least if the local luminosity function keeps relatively flat at its faint end. Various explanations have been proposed, resorting to either density evolution [1] or to luminosity-dependent evolution [2], or to a non-zero cosmological constant [3]; on the other hand, Gronwall and Koo [4] obtained good fits to the data with a standard photometric evolution model with a SMC extinction law, assuming a strong excess (still consistent with the data) of low-luminosity galaxies over the Schechter luminosity function.

Crucial constraints, concerning in particular the effects of dust in high-z galaxies [5], come from observations at infrared wavelengths. A great observational stride occurred thanks to the impressively fast advances in infrared array technology, which have already made it possible to reach a limiting magnitude $K = 23$ [6, 7], *i.e.* surface densities $\simeq 2 \times 10^5$ degrees^{-2} close to those of the deepest optical surveys.

Unlike optical counts, which are highly responsive to young stellar populations, hence prone to very uncertain K-corrections and biased against early-type galaxies, near-infrared counts are much less sensitive to the detailed star formation history. By allowing a more straightforward interpretation, they are going to set much tighter constraints on galaxy evolution.

The extremely interesting new result was that counts in the K band show a remarkable flattening below $K \simeq 20$, at variance with the steep counts observed in the optical.

In the far IR, the first indication that the IRAS galaxy population evolves significantly came from 60 μm counts performed at the faintest flux levels [8,9] and at medium sensitivities [10]. The more detailed information made available by redshift surveys [11] suggests a strongly evolving luminosity function, with a luminosity evolution rate comparable to that of quasars:

$$L(z) = L_0(1+z)^{3.3}. \tag{1}$$

The redshift space, however, was sampled by the IRAS survey only to $z \sim 0.2$, not enough to distinguish between luminosity and density evolution. The limited sampled volume also implies that the estimate of the evolution rate in eq. (1) is possibly affected by large-scale structure. An underdensity by a factor of roughly two in the local universe has been invoked to interpret the very steep counts of galaxies in the optical at $B < 18$, in particular from the APM survey in the southern sky [12].

Near- and far-IR selections emphasize quite different physical processes in galaxies: photospheric emission of red giant stars, mostly unaffected by diffuse dust, in the K band, and dust re-radiation powered by young stellar populations at far-IR wavelengths. To best exploit the information content of the two bands, we need a tool to relate the properties of the ISM (gas fraction, metal abundance and dust content) with those of the stellar populations. The next chapter is devoted to discuss such a tool.

2. – A comprehensive view on galaxy evolution: The basic recipes

Evolutionary population synthesis (EPS) models which account for dust effects have been worked out by [13,14]. Given their large spectral coverage, from ultraviolet to 1 mm, these models allow a synoptic view of data relevant to understand galaxy evolution. They deal, in a self-consistent way, with chemical and photometric evolution of a galaxy over four decades in wavelength. The synthetic spectral energy distribution (SED) incorporates stellar emission, internal extinction and re-emission by dust. The stellar contribution, including all evolutionary phases of stars born with different metallicities, extends up to $25\ \mu$m. Dust includes a cold component, heated by the general radiation field, and a warm component associated with HII regions. Emission from polycyclic aromatic hydrocarbon molecules (PAH) and from circumstellar dust shells are also taken into account.

The star formation rate (SFR) and the initial mass function (IMF) are the basic input functions. The most critical parameter, whose variation is able to account for the whole Hubble sequence, is the initial value of the SFR, ψ_0. Low values of ψ_0 correspond to a SFR slowly decrease with time, the standard scenario for late-type systems; high values of ψ_0 provide a drastically different behaviour, due to the fast decrease of the gas fraction, hence of the SFR: this corresponds to early-type systems.

Models successfully match the SED of local galaxies of different morphological type over four decades in frequency [13, 14]. In the following we will refer to models computed with a Salpeter IMF and a SFR depending on a power law of the mass of gas: SFR $\propto M_{\rm gas}^n$, with $n = 0.5$. This corresponds to a quick metal enrichment and a prompt contamination by dust of the interstellar medium: early-type systems become bright far-IR sources given the high optical depth provided by these models during their initial evolution.

3. – Observational tests of the evolution

The evolution with cosmic time of stellar populations in galaxies can be directly investigated by looking at the spectral energy distribution (SED) of galaxies at different redshifts. "Normal" high-z galaxies, however, proved to be remarkably elusive: none of the 100 (out of a total of 104) galaxies with measured redshift in the sample of Colless *et al.* [15], complete to $B = 22.5$, has $z > 0.7$; the highest redshift in the complete $B < 24$ sample of Cowie *et al.* [16] is $z = 0.73$; the measured redshifts of near-IR selected galaxies down to $K = 20$ [17] (nearly 100% complete at $K < 18$ and $\sim 70\%$ complete at K=19–20) are $\lesssim 1$, with the exception of one object at $z = 2.35$.

So far, the only effective method to find high-z galaxies has been optical identifications of radio sources [18]; far-IR/sub-mm observations of these objects are providing extremely important indications on the properties of young galaxies.

In the following, we will briefly review recent observational results in the near-IR and far-IR/sub-mm bands.

3˙1. *Near-IR–selected galaxy samples.* – Impressive results have been recently obtained by the IfA team at Hawaii [17], [19]. Figures 1 and 2 compare the data of [17] with synthetic colours yielded by models described in the previous section.

We note that evolutionary effects in the spectra of early-type systems cannot be neglected at $z \geq 1$; the use of template SED's of local objects to infer photometric redshifts of galaxies lacking spectroscopy may be misleading. We have compared, in particular, the colours of the 16 unidentified galaxies in the K-band selected sample by [17] and found

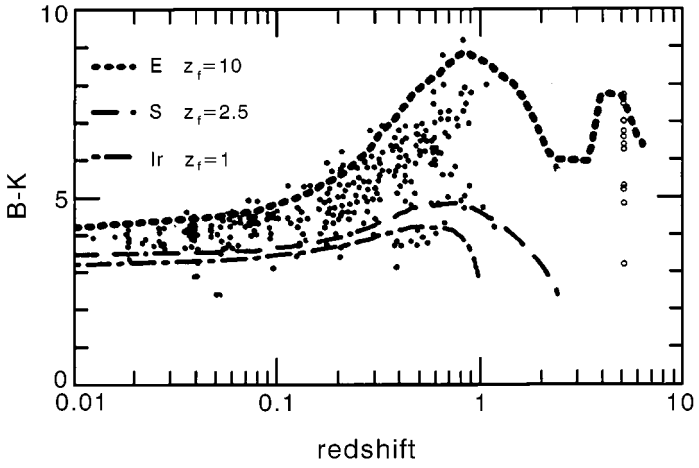

Fig. 1. – Colour-redshift relationships predicted by photometric evolution models described in sect. **2** for galaxies of different morphological types assumed to start their star formation at the redshifts $z_{\rm f}$ indicated, compared with data of [17]. The open symbols show the colours of galaxies lacking redshift measurements, plotted at a nominal $z = 5$.

that most of them are likely to be at $z > 1$. A higher SFR implies bluer colours at $z > 1$ than expected by simply reshifting local SEDs.

Note, in any case, that both the red peak in the colours at $z \simeq 1$ and the subsequent blueing, strongly depend on the adopted cosmological model; in particular, colours $(I - K) > 5$ are difficult to obtain in a closed world model.

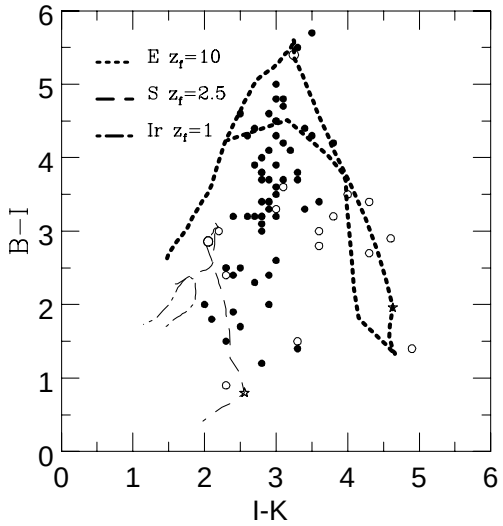

Fig. 2. – Colour-colour plots for intermediate redshift ($0.5 \leq z \leq 1$) galaxies (filled circles) and of candidate high-z galaxies (open circles) in the sample of [17]. The lines show predictions of the same models as in fig. 1. The circle and the star mark the synthetic colours at $z = 1$ and $z = 2$, respectively, of galaxies of each morphological type.

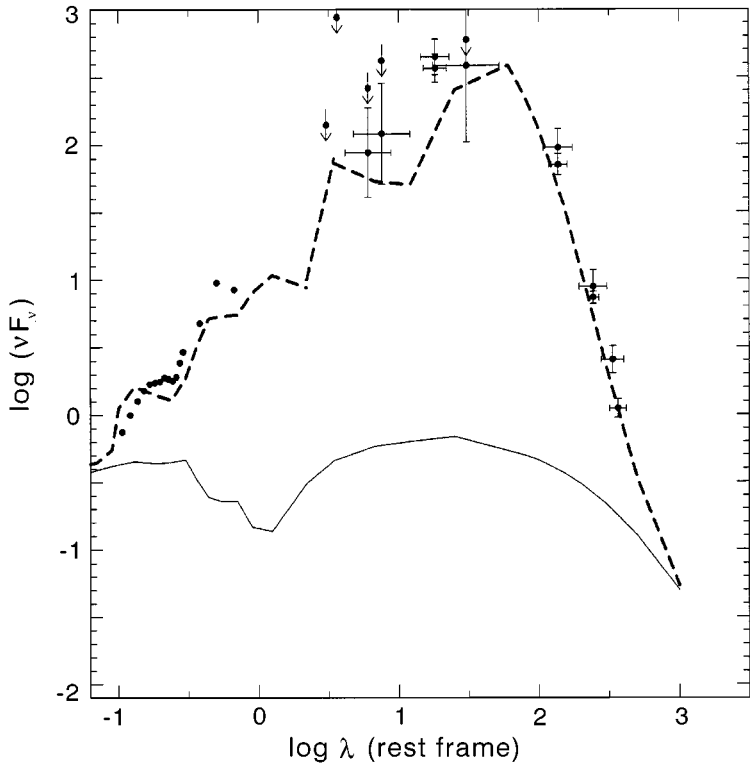

Fig. 3. – Spectral energy distribution of the hyperluminous galaxy IRAS F10214 + 4724 at $z = 2.29$ (see [20] for details and references). A non-thermal contribution having a spectrum equal to the mean spectrum of Seyfert 1 nuclei [21] and accounting for 60% of the rest-frame flux at $\lambda = 0.1$ μm, has been included.

Indications in favour of a merging-driven evolution, in which galaxies become more numerous but less luminous in the past, have been found, *e.g.*, by [19]. Alternatively, we find that, taking into account the combined spectral effects of the evolving stellar populations and of extinction by dust, all the basic statistical properties of K-band selected galaxies can be explained by pure luminosity evolution of the observed local luminosity functions. We account, in particular, for the blueing trend observed at $K > 19$ and $z \sim 1$ as an evolutionary effect due to the higher SFR, rather than a change in the galaxy population mixture.

A world model with $q_0 = 0.15$ and $z_{\rm form} = 7$ for early-type and $z_{\rm form} \simeq 2$ for late-type galaxies is indicated by fits of the observed counts, local luminosity functions, redshift and colour distributions.

3˙2. *Far-IR and radio-selected samples.* – Early-type models including a dusty phase during their initial evolution also match successfully the observed spectrum of the ultraluminous galaxy IRAS F10214 + 4724 at $z = 2.29$ [20]. In fig. 3 we compare the observed SED with model predictions; a non-thermal contribution [21] accounting for 60% of the rest-frame flux at $\lambda = 0.1$ μm has also been included.

Figure 4 (panels a-c) compares, in the rest-frame, the data on three distant radio galaxies having recent sub-mm measurements or upper limits [22,23] with our synthetic SEDs.

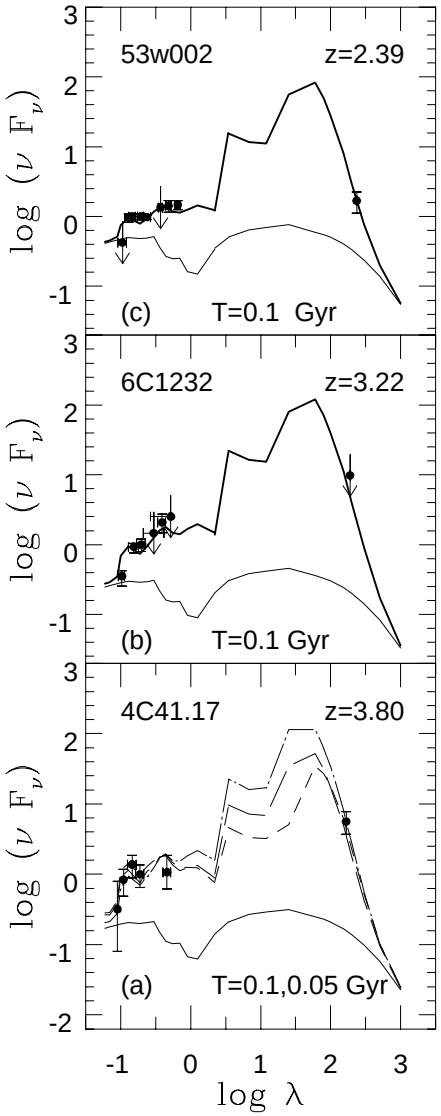

Fig. 4. – Fits to the SEDs of three high-z radiogalaxies. The ages of the models are specified in each panels. The lower thin curves show the assumed nuclear contributions.

The available data can be fully accounted for by "opaque" models like those used by [20] to fit the spectrum of IRAS $\mathrm{F}10214+4724$. The inferred galactic ages are ≤ 0.1 Gy, thus alleviating the problem of galaxy ages uncomfortably high in comparison with the age of the universe as well as the difficulty to understand the alignement between optical/infrared continua and the (presumably short-lived) radio jets [24].

4. – IR **emission of** AGNs

The infrared luminosity is often a significant fraction of the bolometric luminosity of AGNs. In the case of radio-quiet AGNs, the origin of the IR emission is still debated,

although in the last few years observational evidence has accumulated in favour of dust reprocessing of the primary optical-UV emission. Major issues in favour of dust emission are (cf. [21] and references therein): i) the observed SEDs showing a steep rise of the submillimetric continuum between 1000 and 100 μm which is far too steep for any current non-thermal model, and a local minimum in νF_ν at $\lambda \simeq 1\,\mu$m, which is naturally explained by models wherein dust radiates with a limiting sublimation temperature $T_{\rm s} \sim 1500$ K; ii) the IR variability and its relationship with UV and optical variability with delays among different bands which are easily interpreted in dust models; and iii) the observed low level of polarization.

Presence of optically thick dust with azimuthal symmetry has been also advocated to explain the observed difference between broad- and narrow-line AGN in the framework of unified schemes (see [25] for a comprehensive review). As is well known, spectropolarimetric data have shown that broad lines are also visible in polarized light in narrow-line nuclei. More recently, infrared spectroscopy in the near-IR revealed the presence of broad components in hydrogen IR lines (see, *e.g.*, [26]), suggestive of the possibility of a direct view of broad-line regions in the IR. Less direct evidence of dust around active nuclei has been found through studies of ionization cones in several Seyfert 2 galaxies, which demonstrate that the gas in the host galaxies sees anisotropic ionizing sources. Also X-ray observations revealed high absorbing columns ($N_{\rm HI} \sim 10^{23}$– $10^{25}{\rm cm}^{-2}$) in many Seyfert 2 galaxies, whereas Seyfert 1 X-ray spectra exhibit moderate-to-low absorption.

Structure and emission of dust tori or warped discs around AGNs have been investigated by several authors [21, 27]. In the case of tori, dust is assumed to have standard galactic composition, size distribution and sublimation temperature. Various structures have been investigated depending on equatorial optical depth, covering factor, shape, radial and axial dust density distribution. The models can be broadly divided in two classes. A first one includes models with extremely high optical depths ($A_V \geq 500$) and extremely compact structure (the ratio of the outer $r_{\rm out}$ to the inner radius $r_{\rm in}$ of the dust distribution ranges from few to several tens). Typical problems of these models are that torus emission does not fit the observed spectra and surface brightnesses of Seyfert 1 and 2 unless additional dust components are invoked (see, *e.g.*, [27]).

The second family of models requires less extreme optical depth ($A_V \sim 100$) and more extended tori ($r_{\rm in}/r_{\rm out} \sim$ few hundreds) [21]. These models have the nice properties of fitting the observed SEDs and of predicting a size of the region emitting at mid IR extending over several tens of parsecs in agreement with the observations. Moreover the predicted anisotropy of the 10μm emission is within the limits required by the comparison of the luminosity functions of type 1 and type 2 Seyferts [28].

If the latter models hold, the 12 μm luminosity functions of the two Seyfert types [29] and the statistics of the ratio of hard X-ray to 12 μm fluxes [30] indicate that not many hidden AGNs exist. At most 20% of Seyfert 1 and 50% of Seyfert 2 galaxies could have been misidentified as non-active. Moreover the non-linear relation $L_{12} \propto L_{\rm HX}^{0.7}$ suggests that the covering factor decreases with increasing source power [30].

5. – Contributions to the background flux

In the absence of dust extinction, the diffuse radiation generated by early stellar nucleosynthesis is expected to peak in the near IR and to have a bolometric intensity:

$$I_{\rm bol} = \frac{0.007 c^2 \rho f_{\rm m}}{4\pi(1+z_{\rm f})}\ {\rm erg\,cm^{-2}\,s^{-1}\,sr^{-1}}, \tag{2}$$

where z_f is the galaxy formation redshift, ρ is the density of the processed material to produce a mass fraction f_m of metals. Dust eventually re-radiates this energy at longer wavelengths.

Estimates of the IR background intensity have been attempted in the near-IR and sub-mm bands, where the bright foreground emissions from the Galaxy and Inter-Planetary Dust (IPD) are at a minimum. In any case, careful modelling and subtraction of foregrounds is necessary. A summary of recent results is shown in fig. 5.

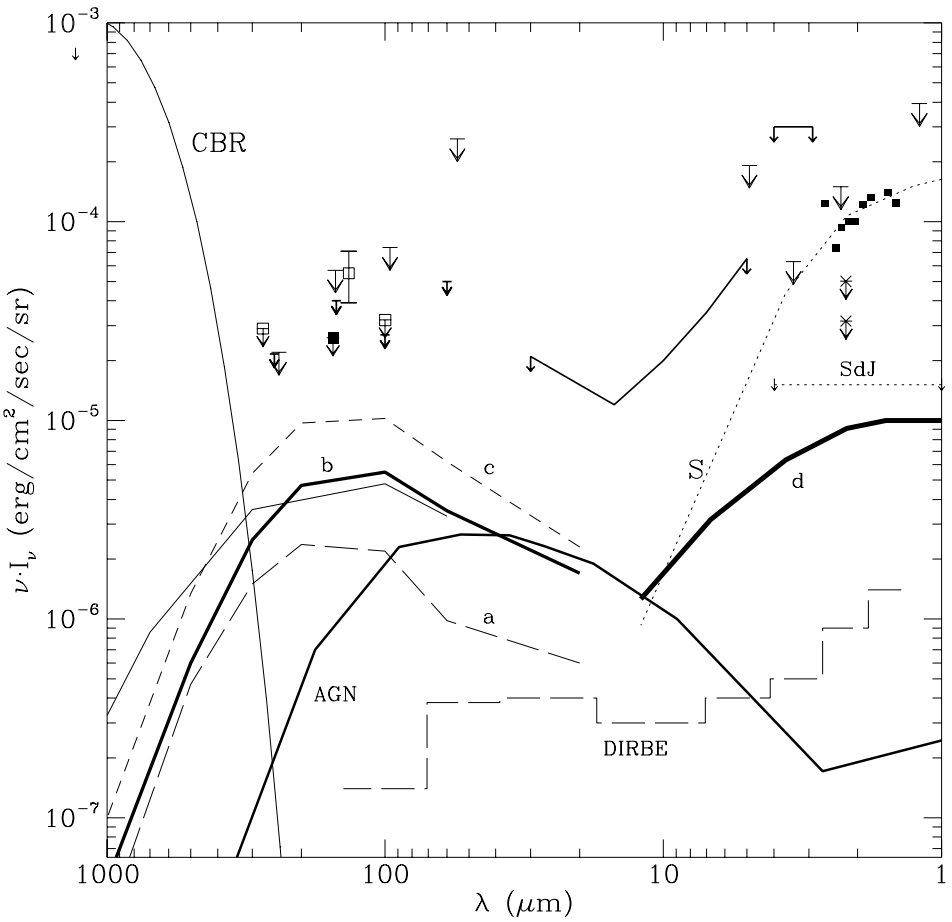

Fig. 5. – Extragalactic background light at IR to sub-mm wavelengths. Curve "a" corresponds to no evolution, curves "b" and "c" to moderate or strong extinction, respectively, of early type galaxies during early evolutionary phases; curve "d" is the integrated starlight of distant galaxies in the near-IR, derived from models fitting the deep K-band counts. Curve "S" shows the contribution of stars in our own Galaxy, at high galactic latitudes. The curve labelled "AGN" shows the somewhat extreme estimate of the possible AGN contribution to the background described in subsect. 5˙2. The DIRBE sensitivity as function of λ is also shown.

5˙1. *The near-IR background.* – The thick solid line labelled "d" in fig. 5 shows the contribution of starlight as implied by models described in subsect. **3˙1**. This estimate is quite a robust one, constrained as it is by existing deep counts of galaxies in K band. The predicted spectral shape is also well constrained up to $\lambda \sim 5\mu$m by our present understanding of photometric evolution.

The tightest observational limits come from observations of very high-energy (TeV) γ-rays in the spectra of the BL Lac object Mkn 421 and follow from the fact that a flux of extragalactic γ-rays is attenuated by interactions with ambient photons leading to the production of electron-positron pairs [31], [32]. These limits are consistent with the near-IR background mostly originating from ordinary stellar processes in galaxies.

Also reported in fig. 5 is the estimated final sensitivity of DIRBE on COBE, which, in principle, would allow accurate determinations of the extragalactic background flux from 1 to 200 μm. As already mentioned, however, the main limiting factor are uncertainties in the estimates of the foreground components.

5˙2. *The far-IR/sub-mm background.* – In fig. 5, the lines labelled "a", "b", "c" show predictions of detailed evolutionary models, while the thin line is based on simpler kinematical prescriptions fitting the $60\,\mu$m statistic [33]. We see an appreciable latitude in such predictions. Note, however, that the extreme curves "a" and "c" bound a sort of conservative "allowed region", the former curve, assuming no evolution, being already inconsistent with $60\,\mu$m counts, the latter corresponding to an evolution rate probably inconsistent with the observed lack of high-z galaxies among faint IRAS sources [9].

The prediction of the kinematic model implies a higher flux level at mm wavelenghts as it assumes a dust temperature distribution constant with time. Physical models predict a lower mm background because dust gets warmer in the past, following the increase of the SFR and of the average radiation field in galaxies.

The various observational limits, set by re-analyses of IRAS survey data [11], by the COBE-FIRAS all-sky spectra deconvolved from the Galaxy emission [34] and by rocket observations [35], are within a factor of a few of the expected extragalactic flux. The latter turns out to be very close to the sensitivity limits of current observations.

5˙3. *A mid-IR background from hot dust in AGNs?* – At the minimum between the predicted *starlight* background in the near-IR and the *dust re-radiation* feature in the far IR, there is a spectral region ($5 < \lambda < 20\,\mu$m) in which properties of even local galaxies are very poorly known (essentially because of the poor sensitivity of IRAS at these wavelengths). Existing data suggest, in any case, that the integrated emission of normal galaxies should keep below 3×10^{-6} erg cm^{-2} s^{-1} sr^{-1}, unless dust with implausibly high temperature characterizes the early evolution phases.

As previously discussed, dust hot enough to emit at these wavelengths is likely to be present in AGNs. The corresponding contribution to the mid-IR background is set by the convolution of the local IR volume emissivity of AGNs with their evolution rate. We report in fig. 5 (line marked AGN) a crude estimate based on the $12\,\mu$m luminosity function of type 1 and 2 Seyfert galaxies by [29] and an evolution rate equal to that of optical QSOs (eq. (1)), extrapolated to $z_{\max} = 4$ with $q_0 = 0.05$. The adopted IR spectra for the two AGN types are the average SED of Seyfert 1 nuclei and the SED of NGC 1068 [21]. The IR luminosity function of Seyferts 2 has been renormalized upwards by a factor 4 to account for the fraction of optically undetected, dust extinguished AGNs predicted by the unified AGN model. We see that, with these somewhat extreme ingredients, the contribution of dusty AGNs in the range 10–50 μm may exceed those of other galaxy populations.

REFERENCES

[1] ROCCA-VOLMERANGE B. and GUIDERDONI B., *Mon. Not. R. Astron. Soc.*, **247** (1990) 166.
[2] BROADHURST T. J., ELLIS R. S. and SHANKS T., *Mon. Not. R. Astron. Soc.*, **235** (1988) 827.
[3] FUKUGITA M., TAKAHARA F., YAMASHITA K. and YOSHII Y., *Astrophys. J.*, **361** (1990) L1.
[4] GRONWALL C. and KOO D. C., *Astrophys. J.*, **440** (1995) L1.
[5] FRANCESCHINI A., MAZZEI P., DE ZOTTI G. and DANESE L., *Astrophys. J.*, **427** (1994) 140.
[6] GARDNER J. P., COWIE L. L. and WAINSCOAT R. J., *Astrophys. J.*, **415** (1993) L9.
[7] DJORGOWSKI S. *et al.*, *Astrophys. J.*, **438** (1993) L13.
[8] HACKING P. and HOUCK J. R., *Astrophys. J. Suppl.*, **63** (1987) 311.
[9] ASHBY M. L. N., HACKING P. B., HOUCK J. R., SOIFER B. T. and WEISSTEIN E. W., *Astrophys. J.*, 456 (1996) 428.
[10] SAUNDERS W., ROWAN-ROBINSON M., LAWRENCE A., EFSTATHIOU G., KAISER N., ELLIS R. S. and FRENK C. S., *Mon. Not. R. Astron. Soc.*, **242** (1990) 318.
[11] OLIVER S. J. *et al.*, *Proceedings of the 35th Herstmonceaux Conference "Wide-Field Spectroscopy and the Distant Universe"*, edited by S. J. MADDOX and A. ARAGON-SALAMANCA (World Scientific) 1995.
[12] ELLIS R., preprint (1995).
[13] MAZZEI P., XU C. and DE ZOTTI G., *Astron. Astrophys.*, **256** (1992) 45.
[14] MAZZEI P., DE ZOTTI G. and XU C., *Astrophys. J.*, **422** (1994) 81.
[15] COLLESS M. M., ELLIS R. S., TAYLOR K. and PETERSON B., *Mon. Not. R. Astron. Soc.*, **261** (1993) 19.
[16] COWIE L. L., SONGAILA, A. and HU E. M., *Nature*, **354** (1991) 460.
[17] SONGAILA A., COWIE L. L., HU E. M. and GARDNER J. P., *Astrophys. J. Suppl.*, **94** (1994) 461.
[18] MCCARTY J. P., *Annu. Rev. Astron. Astrophys.*, **31** (1993) 639.
[19] COWIE L. L., GARDNER J. P., SONGAILA A., HODAPP K. W. and WAINSCOAT R. J, *Astrophys. J.*, **434** (1994) 114.
[20] MAZZEI P. and DE ZOTTI G., *Mon. Not. R. Astron. Soc.*, **266** (1994) L5.
[21] GRANATO L. and DANESE L., *Mon. Not. R. Astron. Soc.*, **268** (1994) 235.
[22] EALES S. A., RAWLINGS S., DICKINSON M., SPINRAD H., HILL G. J. and LACY M., *Astrophys. J.*, **409** (1993) 578.
[23] HUGHES D., DUNLOP J., RAWLINGS S. and EALES S., paper presented at the *European and National Astronomy Meeting, Edinburgh* (1994).
[24] EISENHARDT P. and CHOKSHI A., *Astrophys. J.*, **351** (1990) L9.
[25] ANTONUCCI R., *Mon. Not. R. Astron. Soc.*, **31** (1993) 473.
[26] GOODRICH R. W., VEILLEUX S. and HILL G. J., *Astrophys. J.*, **422** (1994) 52.
[27] PIER E. A., KROLIK J. H., *Astrophys. J.*, **401** (1993) 99.
[28] GIURICIN G., MARDIROSSIAN F. and MEZZETTI M., *Astrophys. J.*, 446 (1995) 550.
[29] RUSH B., MALKAN M. A. and SPINOGLIO L., *Astrophys. J. Suppl.*, **98** (1993) 1.
[30] BARCONS X., FRANCESCHINI A., DE ZOTTI G., DANESE L. and MIYAJI T., *Astrophys. J.* 455 (1995) 480.
[31] STECKER F. W. and DE JAGER O. C., *Astrophys. J.*, **415** (1993) L71.
[32] DWEK E. and SLAVIN J., *Astrophys. J.*, **436** (1994) 696.
[33] FRANCESCHINI A., TOFFOLATTI L., MAZZEI P., DANESE L. and DE ZOTTI G., *Astrophys. J. Suppl.*, **89** (1991) 285.
[34] WRIGHT E. L. *et al.*, *Astrophys. J.*, **420** (1994) 450.
[35] KAWADA M. *et al.*, *Astrophys. J.*, **425** (1994) L89.